ARMA 25–813

Quantifying Topographic Influences on Rockfall Trajectories in Open Pit Mines Using Stochastic Rockfall Modeling

McNabb, J.C.
University of Arizona Geotechnical Center of Excellence, Tucson, Arizona, U.S.A.
Potter, J.J. and Restrepo, J.A.
University of Arizona Geotechnical Center of Excellence, Tucson, Arizona, U.S.A.
Warren, S. N.
National Institute for Occupational Safety and Health, Spokane, WA, U.S.A.
Ryan, T. M.
Call and Nicholas Inc. Tucson AZ, U.S.A.
Luxbacher, K. D.
University of Arizona Department of Mining and Geological Engineering, Tucson, Arizona, U.S.A.

This paper was prepared for presentation at the 59th US Rock Mechanics/Geomechanics Symposium held in Santa Fe, New Mexico, USA, 8-11 June 2025. This paper was selected for presentation at the symposium by an ARMA Technical Program Committee based on a technical and critical review of the paper by a minimum of two technical reviewers. The material, as presented, does not necessarily reflect any position of ARMA, its officers, or members. Electronic reproduction, distribution, or storage of any part of this paper for commercial purposes without the written consent of ARMA is prohibited. Permission to reproduce in print is restricted to an abstract of not more than 200 words; illustrations may not be copied. The abstract must contain conspicuous acknowledgement of where and by whom the paper was presented.

ABSTRACT: Rockfall remains one of the most critical and least understood hazards faced in open pit mining. The factors controlling when and where rockfalls occur are abundant and highly variable site to site, hindering development of effective tools for proactive rockfall hazard mapping at scales relevant to mining operations. Observations from controlled rockfall tests on mined pit slopes conducted by NIOSH support previous studies, highlighting the significant influence of sub-bench-scale topographic features on rockfall trajectories. Specifically, bench face protrusions at a lower angle than the overall bench face, which tend to "launch" rocks into trajectories with greater horizontal velocity components. While often described by previous researchers, the phenomenon is rarely evaluated quantitatively. The influence of launch features on rockfall trajectories and kinetics can be evaluated using detailed stochastic 2D rockfall modeling. This study presents the preliminary results of such modeling, which focuses on primary rockfall impact distances beneath these launch features using 27 systematic combinations of launch feature widths, angles, and heights above the catch bench, with model parameters calibrated to the NIOSH rockfall tests. This analysis serves as a critical first step in creating generalizable, predictive rockfall hazard maps incorporating launch feature geometries mapped from as-built high-resolution pit slope surveys.

1. INTRODUCTION

Increasing demands for critical minerals have necessitated deeper and steeper open pit mine designs to access resources while limiting the expansion of mining footprints. Consequently, significant advancements in slope monitoring have been made to ensure these slopes are mined and maintained safely, efficiently, and economically (Sharon & Eberhardt, 2020). The proliferation of technologies such as ground-based radar and drones have facilitated rapid and accurate identification of large-scale slope movements well in advance of total collapse, allowing for advanced observational mining practices where operations can coexist with active, well-understood slope movements (Chandarana et al., 2016). Despite these advancements, rockfall remains a poorly mitigated and frequent hazard in large open pits. The time between an initial detectable rockfall movement and a life-threatening rockfall hazard occurs in the order of seconds to minutes, compared with detectable precursory signs of large-scale slope collapses which generally span 10's of minutes to months or even years (Williams et al., 2021). Recent advancements utilizing doppler ground-based radars and thermal imaging technologies yield promising results for real-time tracking and alarming for rockfall, and for longer-term analyses such as rockfall source area mapping, runout distance tracking, and rockfall retention performance (Carlà et al., 2024; Wellman et al., 2024; Potter et al., 2024). However, in the case of rapidly evolving rockfall hazards, real-time alerts should serve as a last-resort mitigation strategy that bolsters a proactive, robust understanding of likely rockfall hazard areas.

Rockfall is a complex phenomenon, with numerous variables influencing their timing, trajectory, and kinetics. While this complexity creates challenges for accurately predicting when, where, and how rockfall will occur, previous and ongoing work has begun to tackle these temporal, spatial, and mechanistic uncertainties. Recent studies have evaluated the temporal relationships between external forces and rockfall initiation, such as meteorological events, with good results, suggesting that factors such as precipitation, freeze-thaw cycles, and solar irradiation are some of the leading drivers of increased rockfall frequency (Macciotta, 2019; Nigrelli et al., 2022). However, more work is required to confidently apply these correlations for temporal rockfall forecasting. Potential rockfall source area identification has been assessed by various methodologies for natural slopes, including terrain analysis that identifies areas of steep rocky outcrops and cliff faces (Loye et al., 2009), kinematic analysis of mapped rockfall discontinuities in steep terrain (Yan et al., 2023), and estimates of regional rock mass strengths based on slope and relief relationships from known rockfall source outcrops (Wang et al., 2021). Due to the nature of open pit mining practices, where rock is blasted, excavated, and the remaining slopes are steep by design, the entirety of an excavated slope likely has potential for rockfall initiation. This, and the time-intensive nature of rockfall modeling, has traditionally led to focused 2D modeling efforts in areas of expected rockfall risk or where worker safety and infrastructure security is critical. Recent advancements in 3D rockfall modeling capabilities allow for the creation of point, line, and plane rockfall source seeders (e.g. Rocscience, 2023), facilitating greater modeling coverage over large areas. However, these models tend to require significant topographic simplification, eliminating important small-scale terrain features that impact rockfall, and can be challenging to calibrate without empirical rockfall observations.

Despite the challenges faced in rockfall forecasting, simplifying assumptions can help converge on generalizable kinematic outcomes for hypothetical rockfalls. For example, the range of possible rockfall trajectories down a slope is limited by physics, the material properties of the slope and falling rock, and the morphology of the slope. Material properties of the slope and rock can be constrained to a range of realistic or published parameters (e.g. Saroglou & Bar, 2017), and other variables such as rock shape and dimension can either be calibrated to historical rockfalls or assumed using broad, reasonable ranges. Slope morphology is highly irregular and variable within and between mine sites, however studies have suggested that specific topographic features are a dominant controlling factor in rockfall trajectories (Pierson et al. 2021; McNabb et al. 2024). In the case of open pit mines, isolated features protruding at lower slope angles than the overall bench face have been shown to translate falling rock into trajectories with greater horizontal velocity components, increasing runout and making them more likely to bypass subsequent benches (Figure 1). Pierson et al. (2001) refer to these as "launch features" (LFs), which occur in various shapes and sizes, each affecting rockfall differently, and commonly result from adverse geological conditions (e.g. discontinuities) and mining practices (e.g. blasting, double-bench mining). McNabb et al. (in review) demonstrated that these LFs, along with bench crest loss, were the primary factors resulting in a hazardous rockfall observed during controlled rockfall testing by NIOSH in an open pit mine. LFs are ubiquitous on mined slopes, and with modern high-resolution topographic surveys are now readily observed, mapped, and analyzed at scales relevant to rockfall assessment.

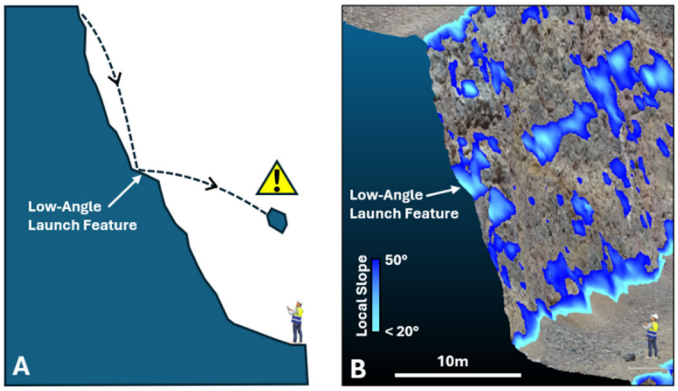

Figure 1. Schematic (A) and real-world (B) examples of launch features occurring on mined bench faces. The example in B is a 3D point cloud from an open pit gold mine in Nevada, U.S.A, with a colored overlay indicating areas of local slope angle between 20° and 50°.

Unlike previous studies that analyze topography to infer areas of likely rockfall initiations, this study focuses on generalizing the effect of small-scale topography (launch features) on rockfall trajectories. The goal is to investigate the fundamental relationships between LF morphologies and the trajectories of rockfall that may encounter them. These relationships will serve as a foundational element in delineating potential rockfall hazard zones imposed by LFs and other topographic features identified from high-resolution topography (e.g. bench crest loss). This work will be combined with concurrent efforts to automate LF mapping and classification from high-resolution point clouds, which will serve as the real-world topographic datasets to which these fundamental relationships can be applied.

2. BACKGROUND

This study stems from an ongoing collaboration with the National Institute of Occupational Safety and Health (NIOSH) and the University of Arizona's Geotechnical Center of Excellence (GCE) to analyze the results of real-

world rockfall tests within open pit mines. The rockfall tests were designed and implemented by NIOSH as part of their ongoing research titled Rockfall Catchment Design and Slope Performance Monitoring at Surface Mines and Quarries, which aims to increase safety in open pit mines and quarries by using empirical rockfall testing data to (1) improve catch bench design criteria and (2) improve slope monitoring guidelines and capabilities (NIOSH, 2022). The GCE became involved in the project in 2021 as part of their study Development and Application of Automated Rockfall Recognition using Computer Vision Approaches applied to Thermal Video from Open Pit Mines (NIOSH contract 75D30122C14875), which aimed to develop a commercially viable rockfall monitoring solution using thermal video and an automated rockfall detection algorithm. The GCE benefitted from the NIOSH rockfall tests by collecting thermal video data during the tests, which unlike natural rockfall, can be assessed in greater detail due to the controlled nature of the tests with respect to rock dimension, fall initiation, and timing.

Data collected during empirical testing included video of the rockfalls in their entirety and high-resolution point clouds of the test highwalls. These data combined allow for high spaciotemporal analysis of rockfall dynamics from initiation to completion. McNabb et al. (in review) presents a detailed analysis of three test rocks, complete with their velocities, kinetics, and trajectories mapped with high precision. They concluded that low-angle topographic protrusions (launch features) and catch bench loss were the primary factors resulting in the most hazardous rockfall dynamics.

3. METHODS

To quantify the effects of launch features on rockfall impact distances, 2D rockfall modeling was conducted using Rocscience's RocFall2 software (Rocscience, 2023). A systematic approach was implemented to evaluate a range of LF dimensions. A 24-m tall, 67° synthetic control (no LFs) bench was generated, mimicking the typical bench design observed during the NIOSH rockfall testing. Then, model scenarios were built from the control bench, which included 27 combinations of three LF angles, three LF widths, and three heights above the catch bench (Figure 2). A horizontal data collection line was placed at the level of the catch bench to measure the impact distance of each simulated rockfall. The data collection line registers a measurement each time a simulated rock crosses it, regardless of the direction it crosses. Therefore, the catch bench shown in the model (Figure 2, in green) was lowered ~8 m beneath the collection line and assigned material parameters to quickly arrest the rockfalls, avoiding erroneous readings from rockfalls bouncing upward off the catch bench and into the data collection line from below. Each simulation involved 10,000 rockfalls initiated 1 m above each LF with varying initial conditions, rock shape, and slope material parameters (Table 1). Rock mass was kept to 100 kg for this preliminary analysis. Initial vertical velocities varied from a minimum of 0 m/s to a maximum that assumes a fall distance equal to the vertical distance from the crest of the bench to the LF midpoint plus another full bench height (Table 1). This assumption is based on observations made during the NIOSH rockfall testing where a singular rockfall was able to bypass a catch bench, allowing it to freefall greater than the height of a single bench, before impacting a LF on the subsequent bench face (McNabb et al., 2024). Initial horizontal velocity ranges were kept constant for each simulation to avoid high initial horizontal velocities that would allow some rocks to bypass the modeled LF. To ensure the entire LF surfaces were impacted by the 10,000 simulated rocks, horizontal line seeders were required for the 1.5 m and 3.0 m LF's, whereas point seeders were adequate for the 0.5 m LF's. The rigid body method of rockfall simulation was chosen for its ability to model the influence of rock shape on rockfall dynamics.

Table 1. 2D rockfall simulation parameters

Bench Face Material	*Rn 0.35 - 0.40, Rt 0.82 - 0.87, Fd 0.44 - 0.60, Fr 0.15 - 0.32
No. of rocks per simulation	10,000
Initial Horizontal Velocity	0 - 1 m/s
Initial Vertical Velocities	0 - 24 m/s (upper bench), 0 - 27 m/s (mid-bench), 0 - 30 m/s (lower bench)
Initial Rotation	-720 deg/sec
Rock Mass	100 Kg
Rock Shapes	Sphere, Circle, Oval (5:6; 2:3), Triangle, Square, Pentagon, Hexagon, Octagon, Egg, Rhombus, Ellipse (5:6; 2:3; 1:2; 1:1), Super Ellipse^4 (5:6 ; 2:3 ; 1:2; 1:1; 5:6; 2:3;1:2), Polygon Triangle, Polygon Square, Polygon Pentagon, Polygon Hexagon, Polygon Octagon, Polygon Rectangle (5:6; 2:3; 1:2)

**Rn = coefficient of normal restitution, Rt = coefficient of tangential restitution, Fd = dynamic friction, Fr = rolling friction*

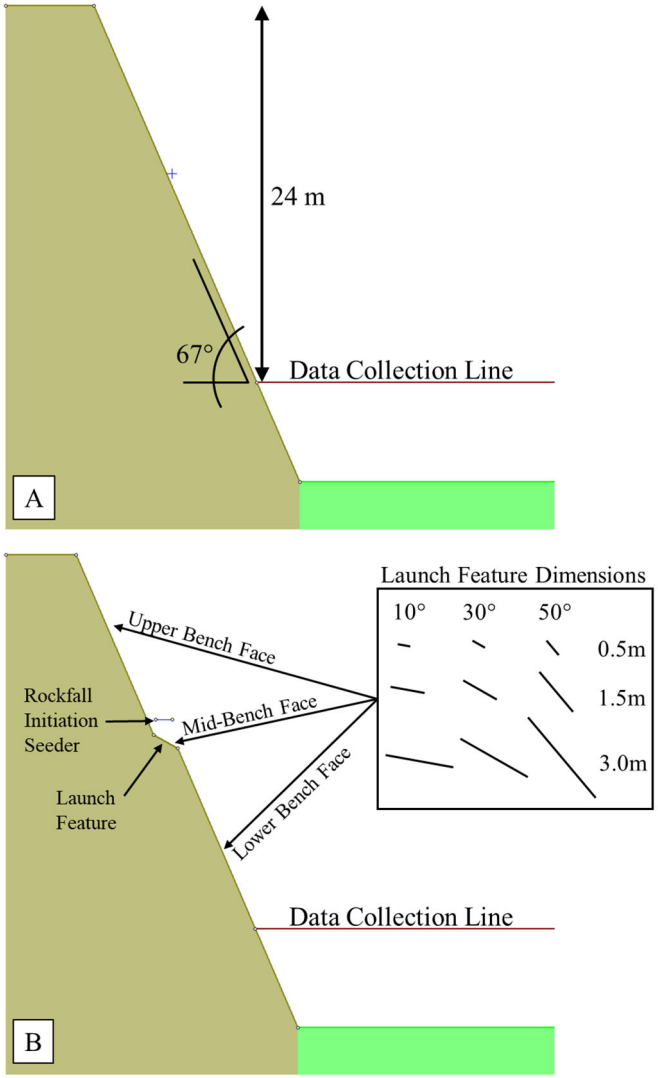

Figure 2. 2D rockfall simulation model setup. A) control bench with no launch feature. B) Example model with a launch feature at the mid-bench level.

4. RESULTS

Full results from the 27 simulations are presented in Table 2 and Figure 3, and a plot showing the 95% impact distance by angle, width, and height above the bench is shown in Figure 4. Of the variables tested in the analysis, LF width proved to have the most significant effect on rockfall impact distance when compared to LF angle and height above the catch bench. Figure 5a shows the 95% impact distance vs LF width for all three LF angles. Overall impact distances decrease with increasing LF width, from higher impact distances at 0.5 m, to lower and similar distances for 1.5 m and 3.0 m. When considering LF angle, the 10° LFs exhibit both the highest impact distances at 0.5 m and the lowest at 1.5 m and 3.0 m compared to the 30° and 50° scenarios, mimicking a power-law decay curve. 30° LFs show decreased impact distances at 0.5 m width compared to 10° LFs, but higher impact distances at 1.5 m and 3.0 m widths, following a similar power-law-like decay, but with a slower decay than 10° LFs. Finally, 50° LFs follow a sub-linear trend (or a fully diminished power-law decay), with no discernible differences in impact distance among the 0.5 m, 1.5 m, and 3.0 m widths. Figure 5b shows the 95% impact distance vs LF angle with each LF width plotted as distinct markers. Overall impact distances show high variance at lower LF angles that converge at higher LF angles. When considering LF width, this plot again shows the highest average impact distances for 0.5 m wide, 10° LFs. With increasing LF angle, the average impact distance for 0.5 m wide LFs drops for 30° and 50° LFs. Conversely, the 1.5 m and 3.0 m wide scenarios show an increasing trend with an increasing LF angle, each with similar values.

Table 2. Full simulation results.

Height Above Catch Bench (m)	Angle (Deg.)	Width (m)	95% Impact Dist. (m)	Max. Impact Dist. (m)
4	NA (Control)		1.5	19.2
4	10	0.5	5.6	25.6
4	10	1.5	2.2	24.7
4	10	3	2.2	25.3
4	30	0.5	5.1	25.7
4	30	1.5	3.5	24.6
4	30	3	3.2	23.2
4	50	0.5	2.6	22.0
4	50	1.5	3.0	23.0
4	50	3	2.7	23.5
12	NA (Control)		1.7	22.9
12	10	0.5	6.2	28.7
12	10	1.5	1.5	26.7
12	10	3	1.6	26.5
12	30	0.5	5.9	28.9
12	30	1.5	3.8	26.6
12	30	3	3.7	25.5
12	50	0.5	4.1	25.5
12	50	1.5	4.0	27.1
12	50	3	3.9	26.8
20	NA (Control)		1.5	23.2
20	10	0.5	3.8	26.9
20	10	1.5	1.3	22.3
20	10	3	1.3	23.0
20	30	0.5	4.3	27.5
20	30	1.5	2.5	27.6
20	30	3	2.4	24.2
20	50	0.5	3.2	25.0
20	50	1.5	3.4	25.4
20	50	3	3.4	27.1

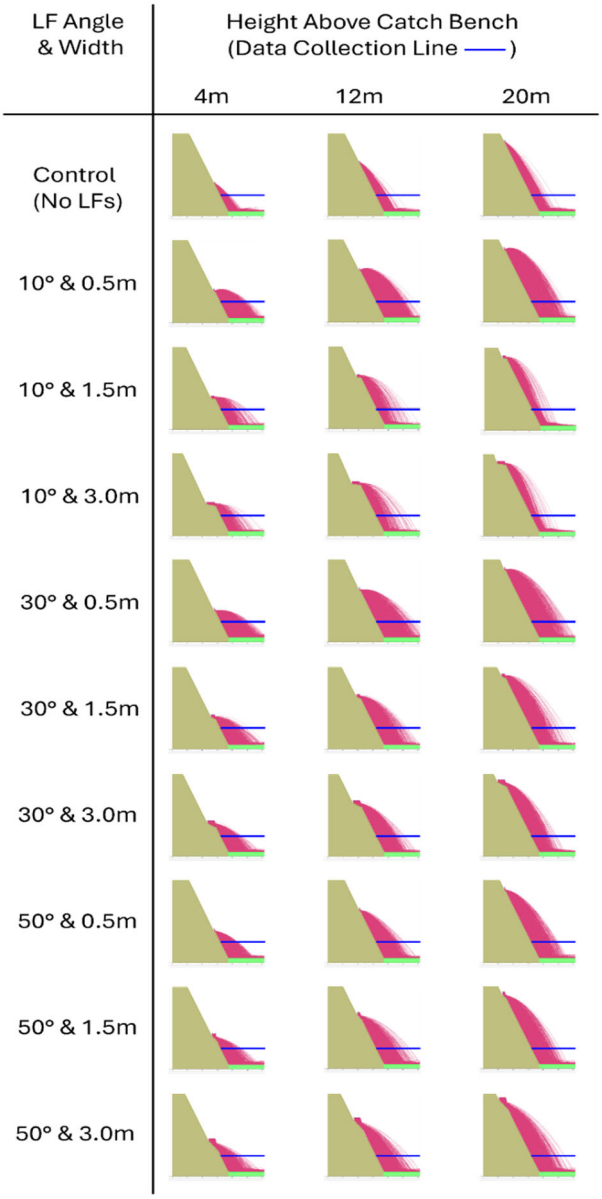

Figure 3. Full simulation results.

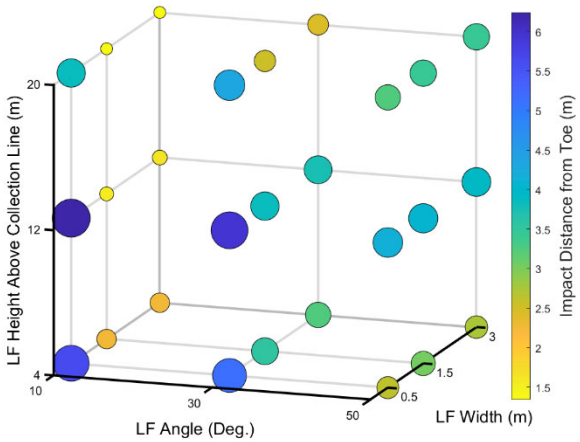

Figure 4. Simulated rockfall impact distances for all modeled scenarios.

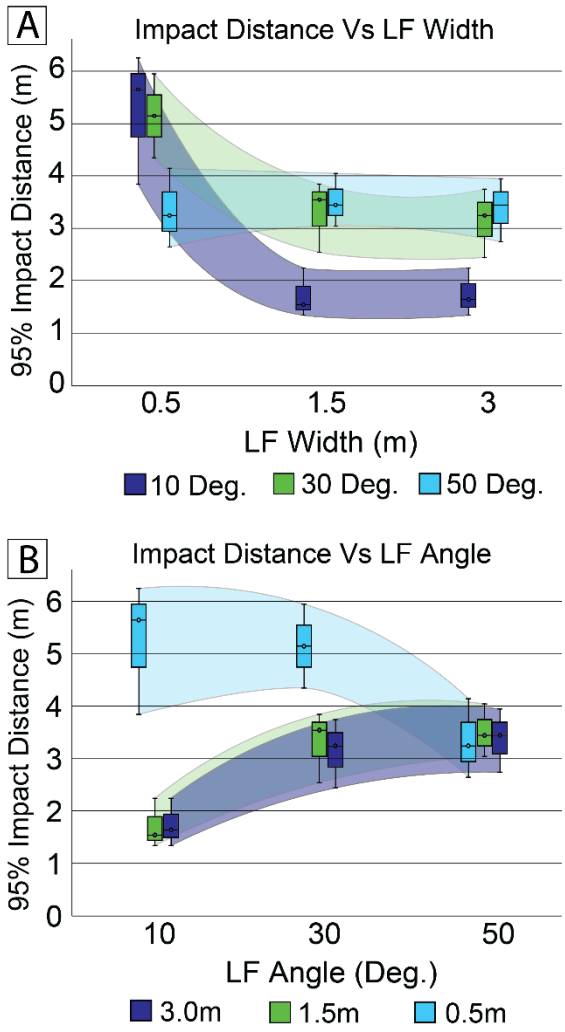

Figure 5. Figure 5. 95% rockfall impact distances vs LF width (a) and LF angle (b).

5. DISCUSSION

Results from this preliminary analysis indicate complex and non-linear, but decipherable relationships between LF width and angle and modeled rockfall impact distances. No apparent trends are observed with respect to LF height above the bench face, given this limited dataset. The strong relationships between LF width and angle with impact distance highlights their potential for predicting impact distances based on these dimensional LF characteristics. While the mechanisms behind these trends are not fully understood at this time, hypotheses can be derived for further evaluation. The trends shown in Figure 5 suggest that as LF angle steepens, the influence of LF angle on impact distance diminishes to a baseline. This is expected as increasing LF angle approaches that of the overall bench face angle. Lower width LFs tend to yield greater impact distances (Fig. 5a), perhaps because a rockfall is likely to impact a narrow LF only once, bouncing off the LF and continuing its fall downslope. Rockfall on wider LFs on the other hand are more likely to experience bouncing, rolling, and sliding if the

trajectories after initial LF impact aren't sufficiently energetic enough to bounce off the LF. Low angle, wide LFs exhibit this dynamic best, where a rock that is not cleared of the LF after the first impact is subject to bouncing/rolling/sliding over the width of the LF prior to continuing its travel.

5.1. Validation With Empirical Rockfall Data

Figure 6 shows an example documented during the NIOSH highwall tests in which test rocks impacted bench face LFs and experienced altered trajectories. The example illustrated by the red star impacted a 0.55-m-wide, 36° LF, which yielded an impact distance of 3.3 m on the catch bench below, which are plotted over the results presented in Figure 5. Two additional examples from the NIOSH tests are plotted in Figure 6 (yellow and pink stars). Comparing these measurements to the preliminary relationships developed in this study shows a reasonable match, however further validation with field observations is required to refine and test these relationships.

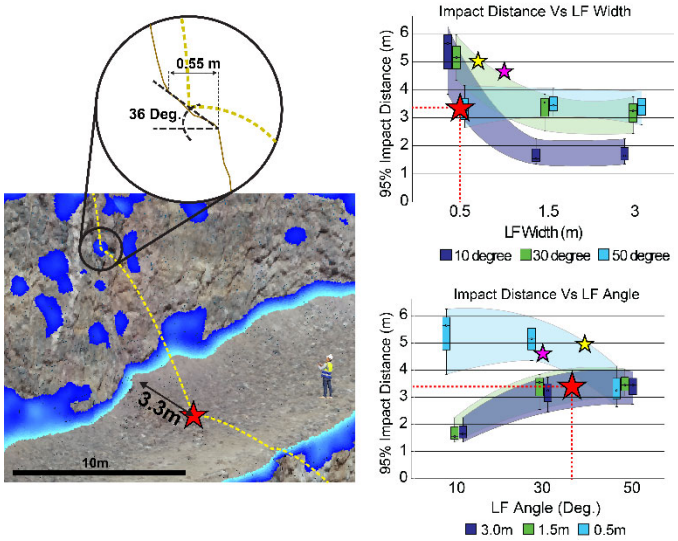

Figure 6. Observed rockfalls from NIOSH test campaign (stars) that impacted launch features plotted over the results from this analysis.

6. FUTURE WORK

The results presented here represent a small subset of potential LF morphologies, but they characterize a range of dimensions commonly observed on mined bench faces. Future efforts will focus on simulating additional combinations of LF angles, widths, and heights above the catch bench, as well as variable rock sizes and initial conditions. Additional validation with empirical rockfall tests is imperative for further model calibration and refinement. 3D rockfall modeling must also be implemented to evaluate dynamics not fully captured in 2D modeling such as lateral dispersion and complex LF morphologies. Other avenues of terrain analysis may also be explored with respect to impact distance, such as bench crest loss and bench face roughness. A key component of rockfall lacking in this study is total rollout distance, which may be explored using empirical rockfall observations, modeled runout distances, and modeled horizontal velocities upon catch bench impact, which can be correlated with both total runout and relative hazard post-impact. If a robust framework for estimating impact distance from topographic measurements can be established, machine learning may be applied to integrate the full process from terrain analysis to hazard area mapping.

7. CONCLUSION

This study presents a preliminary analysis linking topographic launch feature morphologies to initial rockfall impact distances. The results serve as the foundation for future work that will further establish these relationships by evaluating additional parameters such as variable rock size, overall slope angle, broader material properties, and incorporating 3D modeling all in furtherance of generating site-wide rockfall hazard maps based on high-resolution terrain analysis. This work is concurrent with efforts to automate LF detection and characterization from high-resolution topographic surveys, which will serve as the primary data set to which these LF / impact distance relationships will be applied. Additional topographic features known to result in hazardous rockfall trajectories, such as bench loss, will be evaluated and incorporated into the hazard mapping as well, and further validation from empirical rockfall testing will aid in further establishing these relationships.

DISCLAIMERS

The findings and conclusions in this report are those of the author(s) and do not necessarily represent the official position of the National Institute for Occupational Safety and Health, Centers for Disease Control and Prevention. Mention of any company or product does not constitute endorsement by NIOSH, CDC.

ACKNOWLEDGEMENTS

The authors wish to express their sincere gratitude to the member companies of the University of Arizona's Geotechnical Center of Excellence, whose ongoing support, collaboration, and guidance have facilitated this and other innovative research endeavors. Their commitment to advancing geotechnical research for the benefit of the global community is deeply appreciated.

REFERENCES

1. Carlà, T., Gigli, G., Lombardi, L., Nocentini, M., Meier, L., Schmid, L., Wahlen, S., & Casagli, N. (2024). Real-time detection and management of rockfall hazards by ground-based Doppler radar. Landslides, 21(1), 155–163. https://doi.org/10.1007/s10346-023-02144-1
2. Chandarana, U. P., Momayez, M., & Taylor, K. W. (2016). Monitoring and predicting slope instability: A review of current practices from a mining perspective. International Journal of Research in Engineering and Technology, 5(11), 139–151. https://doi.org/10.15623/ijret.2016.0511026
3. Lan, H., Martin, C. D., Zhou, C., & Lim, C. H. (2010). Rockfall hazard analysis using LiDAR and spatial modeling. Geomorphology, 118(1–2), 213–223. https://doi.org/10.1016/j.geomorph.2010.01.002
4. Loye, A., Jaboyedoff, M., & Pedrazzini, A. (2009). Identification of potential rockfall source areas at a regional scale using a DEM-based geomorphometric analysis. Natural Hazards and Earth System Sciences, 9(5), 1643–1653. https://doi.org/10.5194/nhess-9-1643-2009
5. Macciotta, R. (2019). Review and latest insights into rockfall temporal variability associated with weather. Geotechnical Engineering, 172. https://doi.org/10.1680/jgeen.18.00207
6. McNabb, J. C., Meyer, B. J., Potter, J. J., Warren, S. N., & Wagner, D. A. (2024). Rockfall barrier testing in an open pit mine: Comparing empirical and modeled rockfall dynamics. ARMA US Rock Mechanics/Geomechanics Symposium, D021S014R001. https://onepetro.org/ARMAUSRMS/proceedings-abstract/ARMA24/ARMA24/549183
7. McNabb, J. C., Meyer, B. J., Potter, J. J., Warren, S. N., & Wagner, D. A. (in review). Dynamics of controlled rockfall tests in an open pit mine: Implications for bench design and rockfall barriers. University of Arizona Geotechnical Center of Excellence.
8. Nigrelli, G., Chiarle, M., Merlone, A., Coppa, G., & Musacchio, C. (2022). Rock temperature variability in high-altitude rockfall-prone areas. Journal of Mountain Science, 19(3), 798–811. https://doi.org/10.1007/s11629-021-7073-z
9. NIOSH. (2022). Mining Project: Highwall Safety: Rockfall Catchment Design and Slope Performance Monitoring at Surface Mines and Quarries. Retrieved from: https://www.cdc.gov/niosh/mining/researchprogram/projects/project_highwallsafety.html
10. Pierson, L., Gullixon, F., & Chassie, R. (2001). Rockfall catchment area design guide (FHWA-OR-RD-02-04m). Oregon Department of Transportation.
11. Potter, J., Meyer, B., Ross, B., McNabb, J., Keefner, J., Williams, C., Brown, L. D., Prescott, B., & Cabrejo, A. (2024, June). Development of a prototype thermal imaging rockfall detection system. 58th U.S. Rock Mechanics/Geomechanics Symposium. https://dx.doi.org/10.56952/ARMA-2024-1049
12. Rocscience. (2023). RocFall2 (Version 8.024) [Computer software]. Rocscience. https://www.rocscience.com/software/rocfall
13. Saroglou, H., & Bar, N. (2017). Predicting the primary impact and total rollout distances of rockfalls based on cases in quarries and mines in Australia and the United Kingdom. ResearchGate. https://www.researchgate.net/publication/317937417_Predicting_the_primary_impact_and_total_rollout_distances_of_rock_falls_based_on_cases_in_quarries_and_mines_in_Australia_and_the_United_Kingdom
14. Sharon, R., & Eberhardt, E. (2020). Guidelines for slope performance monitoring. CSIRO Publishing.
15. Wellman, E. C., Schafer, K. W., Williams, C. P., Ojum, G. H., Potter, J. J., Brown, L. D., Meyer, B., Ross, B. J., & Kemeny, J. (2024). Observation of rockfall in the thermal infrared. Rock Mechanics and Rock Engineering. https://doi.org/10.1007/s00603-024-04254-1
16. Williams, C., Ross, B., Zebker, M., Leighton, J., Gaida, M., Morkeh, J., & Robotham, M. (2021). Assessment of the available historic RADARSAT-2 synthetic aperture radar data prior to the Manefay Slide at the Bingham Canyon Mine using modern InSAR techniques. Rock Mechanics and Rock Engineering, 54(7), 3469–3489. https://doi.org/10.1007/s00603-021-02483-2
17. Yan, J., Chen, J., Tan, C., Zhang, Y., Liu, Y., Zhao, X., & Wang, Q. (2023). Rockfall source areas identification at local scale by integrating discontinuity-based threshold slope angle and rockfall trajectory analyses. Engineering Geology, 313, 106993. https://doi.org/10.1016/j.enggeo.2023.106993